



BEHAVIORS OF CONCRETE COLUMNS CONFINED WITH BOTH SPIRAL AND FIBER COMPOSITES

Jung-Yoon Lee¹, Young-Jun Oh², Ji-Sun Park³ and Mohamad Y. Mansour⁴

SUMMARY

Concrete columns confined with high-strength fiber reinforced polymer (FRP) composites can enhance the strength as well as the ductility of such structures. In recent years, the use of FRP composites to repair and strengthen existing reinforced concrete (RC) structures has been widely used. When the columns of existing RC structures are wrapped with FRP composites, the core concrete of such columns is confined not only by the FRP composites but also by the existing steel reinforcing ties (or spirals). Therefore, it is necessary to understand correctly the compressive response of concrete confined with both steel spirals and FRP composites in order to predict the behavior of such RC columns.

Since the behavior of the reinforcing steel spiral ties and the FRP composites are different from each other, the behavior of concrete columns confined with both steel spiral and FRP composites is expected to be different from that of concrete columns confined with only steel spiral or FRP composites. In this paper, 24 RC small-scale columns were tested under pure axial compression in order to study the response of RC columns confined with steel spiral ties and FRP composites. Two main parameters were considered in this investigation: the confinement type (one material (FRP composites or steel spiral) versus two materials (FRP composites and steel spiral)) as well as the lateral confining pressure. The test results showed that the compressive response of concrete when confined with two materials (steel spiral ties and FRP) was quite different from the compressive response of concrete when confined with only one material. The study also compares the experimental results to the predicted results obtained using current constitutive relationships found in the technical literature.

INTRODUCTION

Fiber Reinforced Polymer (FRP) is a relatively new class of composite material manufactured from fibers and resins and has proven efficient and economical for the development and repair of new and deteriorating structures in civil engineering. The reasons why FRP are increasingly used as

¹ Assistant Professor, Department of Architectural Engineering, Sungkyunkwan University, South-Korea, jylee@skku.ac.kr

² Structural Engineer, Wonwoo Structural Engineering Co., Seoul, South-Korea

³ Researcher, Building Research Dept., Korea Institute of Construction Technology, Goyang-Si, Gyeonggi-Do, South-Korea

⁴ Research Assistant Professor, Department of Civil & Environmental Engineering, University of Houston, USA

strengthening materials of RC structures are its high strength-to-weight ratio, high corrosion resistance, resulting in easier application in confined space, reduction in labor costs, and ease in site handling.

When wrapped with FRP composites, axially loaded concrete columns exhibit higher strengths and ductility as well as larger energy dissipation capacities than unconfined concrete columns. Thus extensive research was carried out by many investigators; such as Karabinis and Rousakis¹, Campione and Miraglia², Karbhari and Gao³, Ahmad et al.⁴, and Demers M, and Neale⁵, Mirmiran et al.^{6,7} to name a few; to assess and predict the compressive response of concrete columns wrapped with FRP. For example the model proposed by Mirmiran et al.^{6,7} to describe the compressive stress-strain curves of reinforced concrete wrapped with FRP consisted of two regions: the first (initial) region was similar to that of unconfined concrete while the second region considered the effect of FRP confinement and is based on the confinement model originally proposed by Richart et al.⁸. While the model that was originally developed Mander et al.⁹ to predict the compressive stress-strain relationships of concrete confined by steel ties was used by Monti et al.¹⁰ to predict the response of FRP-confined concrete in compression by taking into account the effect of the lateral strain in the model formulation. Similarly to Monti's model, Saafi et al.¹¹ proposed a model in which the effect of the FRP confinement was accounted for by modifying the lateral strain of concrete.

When the columns of existing RC structures are wrapped with FRP composites, the core concrete is confined by two different materials the steel spirals and the FRP composites as shown in Fig. 1(a). If both confining materials exhibit the same behavior, the confining effects (the stress-strain relationships, strength, and ductility) of concrete confined with both materials can be predicted by simply superimposing the lateral confining pressure (f_l) of each material. However, the tensile stress-strain curves of FRP composites and

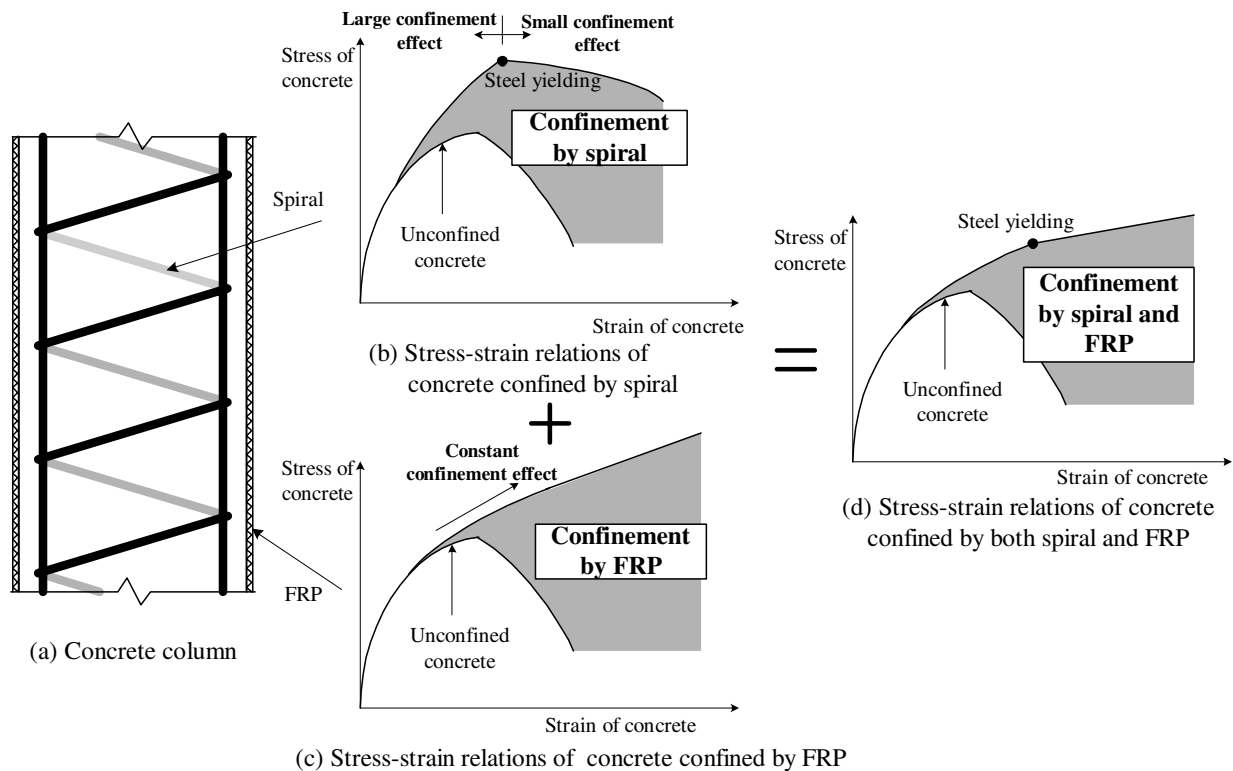


Fig. 1 Stress-strain relationships of confined concrete

steel spirals are different as shown in Fig. 2. The typical stress-strain curves of steel bars consists of an initial linear elastic portion, a yield plateau in which strain increases with little or no increase in stress, and a strain-hardening range. Thus, for the case of steel transverse reinforcement, the constant confining pressure can be assumed when the steel is yielding and the stress-strain relationships of steel-confined concrete gradually decreases after the yielding of the steel as shown in Fig. 1(b).

Unlike the stress-strain curve of steel spiral, FRP exhibits a stress-strain curve: linear elastic up to final brittle rupture when subjected to tension, as shown in Fig. 2. Therefore, the stress-strain relationships of FRP-confined concrete gradually increase and suddenly drop down when FRP composites rupture as shown in Fig. 1(c).

The stress-strain curves of concrete confined with both steel and FRP composites (both material-confined concrete) are influenced with the lateral confining pressures of both confining materials. If the lateral confining pressure (f_{ls}) of steel is smaller than the lateral confining pressure (f_{lf}) of FRP composites, the slope of the stress-strain curves of both material-confined concrete decreases after steel yielding. However, this slope is stiffer than that of the only steel-confined concrete as shown in Fig.1(d). Such confined concrete fails when FRP composites rupture.

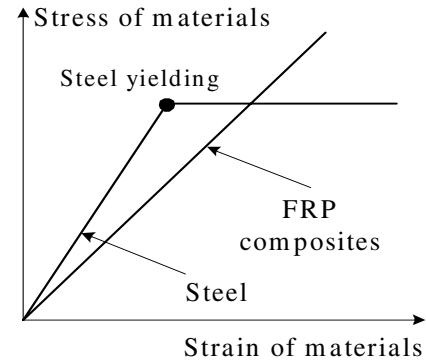


Fig. 2 Stress-strain relationships of steel and FRP composites

When the columns of the existing RC structures are repaired with FRP composites, the core concrete of the columns is confined by both materials (steel spirals / steel hoops and FRP composites) because the FRP composites wrap the existing columns that have been already confined with steel spirals or hoops.

Although many researches have been carried out to study the compressive response of FRP wrapped RC columns, few attempts were done to investigate the effect of FRP composites and steel ties confinement on the axial compressive response of concrete. Thus, in this paper 24 RC small-scale columns were tested under axial compression till failure to assess the effect of both confining materials on compressive response of such columns.

TEST PROGRAM

Test specimens

24 concrete cylinders 150 mm in diameter and 300 mm in height were tested under axial compression till failure. Two parameters were considered in the investigation: the types of confining material (FRP or/and steel ties) and the lateral confining pressure. The 24 cylinders were divided into four series: S0, S6, S4 and S2. Each series consisted of 6 cylinders. While the S0 series was confined only with FRP sheets, the S6, S4 and S2 series were confined with both FRP and steel spiral ties. $\phi 5.5$ bars were used as steel spiral ties in series S2, S4 and S6. The pitch of the steel spiral ties in series S2, S4 and S6 was 20 mm, 40 mm and 60 mm, respectively.

Two letters (S for steel and F for fiber) were used to designate the type of confinement used for each cylinder in each series. The numeric digits next to the "S" and "F" letters were used to designate the pitch of the steel spiral ties in centimeters and the number of FRP layers used, respectively. The "S" letter was used to

designate the steel confinement while the letter “F” was used to designate the FRP composites. The number of FRP layer varied form one cylinder to the other within a series. For example, specimen S0F0 indicates that this cylinder was not confined with steel spiral hoops nor FRP sheets, while S2F4 indicates that this cylinder was confined with steel spiral ties having a pitch of 2 cm and with 4 layers of FRP sheets.

One concrete batch was used to cast the 24 cylinders at the same time. After curing the cylinders, primer was applied to the surface of the cylinders and then the FRP sheets were placed. The average concrete cylinder strength of each specimen at the time of parent cylinder test as well

as the material properties of the steel spirals and the FRP of each cylinder are shown in Table 1. In Table 1, f_c' is the compressive strength of unconfined concrete, ϵ_{co} is the compressive strain of unconfined concrete corresponding to f_c' , f_{sy} is the yield stress of the steel spiral, s is the pitch of the steel spiral, f_{fy} is the tensile strength of CFRP, E_{fs} is the modulus of elasticity of CFRP, and t is the thickness of CFRP.

Fig.3 shows the stress-strain curves of the steel spiral and CFRP composites.

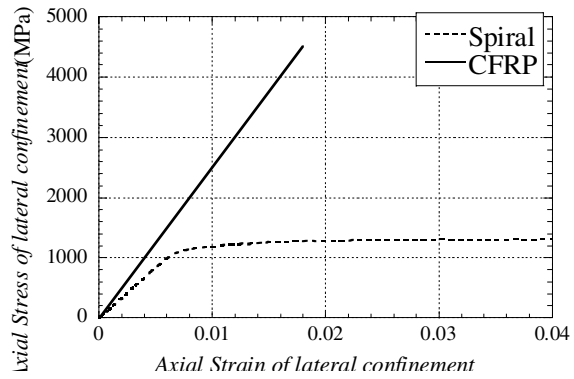


Fig. 3 Stress-strain relationships of confining materials

Table 1 Material properties of cylinders

Specimen	f_c' (MPa)	ϵ_{co} (%)	f_{sy} (MPa)	s (mm)	f_{fy} (MPa)	E_{fs} (GPa)	t (mm)
S0F0	36.2	0.24	1200	1200	-	-	-
S0F1	36.2	0.24	1200	1200	4510	250	0.11
S0F2	36.2	0.24	1200	1200	4510	250	0.22
S0F3	36.2	0.24	1200	1200	4510	250	0.33
S0F4	36.2	0.24	1200	1200	4510	250	0.44
S0F5	36.2	0.24	1200	1200	4510	250	0.55
S6F0	36.2	0.24	1200	60	-	-	-
S6F1	36.2	0.24	1200	60	4510	250	0.11
S6F2	36.2	0.24	1200	60	4510	250	0.22
S6F3	36.2	0.24	1200	60	4510	250	0.33
S6F4	36.2	0.24	1200	60	4510	250	0.44
S6F5	36.2	0.24	1200	60	4510	250	0.55
S4F0	36.2	0.24	1200	40	-	-	-
S4F1	36.2	0.24	1200	40	4510	250	0.11
S4F2	36.2	0.24	1200	40	4510	250	0.22
S4F3	36.2	0.24	1200	40	4510	250	0.33
S4F4	36.2	0.24	1200	40	4510	250	0.44
S4F5	36.2	0.24	1200	40	4510	250	0.55
S2F0	36.2	0.24	1200	20	-	-	-
S2F1	36.2	0.24	1200	20	4510	250	0.11
S2F2	36.2	0.24	1200	20	4510	250	0.22
S2F3	36.2	0.24	1200	20	4510	250	0.33
S2F4	36.2	0.24	1200	20	4510	250	0.44
S2F5	36.2	0.24	1200	20	4510	250	0.55

The lateral confining pressures (f_{ls} and f_{lf}) of steel and CFRP are calculated by Eqs.(1) and (2), respectively. Each lateral pressure of test cylinders is shown in Table 2.

$$f_{ls} = \frac{2A_{sp}f_{sy}}{d_s s} \quad (1)$$

$$f_{lf} = \frac{2f_{ty}t}{D} \quad (2)$$

where, A_{sp} is the sectional area of steel spiral, d_s is the distance between the centres of the spiral, and D is the diameter of cylinder.

In Table 2, while the f_{ls} of all cylinders (S6F1-S6F5) in the S6 series is smaller than f_{lf} , the f_{ls} of the S4 series is approximately the same to f_{lf} of the concrete confined with one layer-sheet

CFRP (S4F1), and the f_{ls} of the S2 series is almost the same to f_{lf} of the concrete confined with two layer-sheet CFRP (S2F2).

Table 2 Lateral pressure of cylinders

Specimen	f_{ls} (MPa)	f_{lf} (MPa)	Specimen	f_{ls} (MPa)	f_{lf} (MPa)
S0F0	0.00	0.00	S4F0	6.25	0.00
S0F1	0.00	6.61	S4F1	6.25	6.61
S0F2	0.00	13.2	S4F2	6.25	13.2
S0F3	0.00	19.8	S4F3	6.25	19.8
S0F4	0.00	26.5	S4F4	6.25	26.5
S0F5	0.00	33.1	S4F5	6.25	33.1
S6F0	3.47	0.00	S2F0	14.81	0.00
S6F1	3.47	6.61	S2F1	14.81	6.61
S6F2	3.47	13.2	S2F2	14.81	13.2
S6F3	3.47	19.8	S2F3	14.81	19.8
S6F4	3.47	26.5	S2F4	14.81	26.5
S6F5	3.47	33.1	S2F5	14.81	33.1

Measurements

The overall dimensions and arrangement of reinforcement are shown in Figs.4 and 5. Six linear displacement transducers (LVDT) were attached to the cylinder as shown in Fig. 4. Three LVDTs were used to measure the axial deformation while the other three were used to measure the lateral deformation of each cylinder. In addition, strain gauges were attached to the surfaces of the steel spiral ties to record the strains of the transverse steel bars.

The load was applied monotonically till failure of the specimen. The applied load, the corresponding LVDTs, and the strain gauge readings were recorded automatically through a data logger at specified load intervals. The test was terminated when the value of the applied load dropped to about 90% of the maximum-recorded load in the post-peak descending branch.

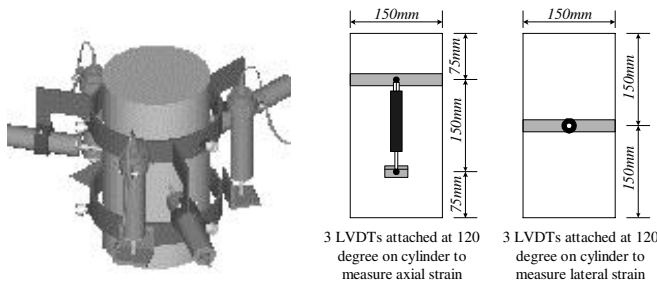


Fig. 4 Locations of LVDTs

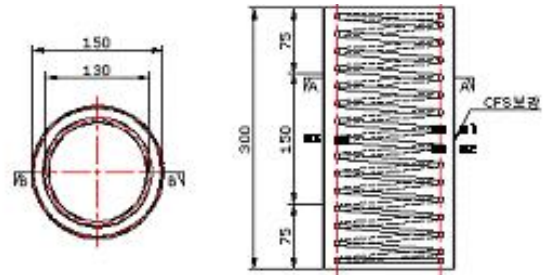
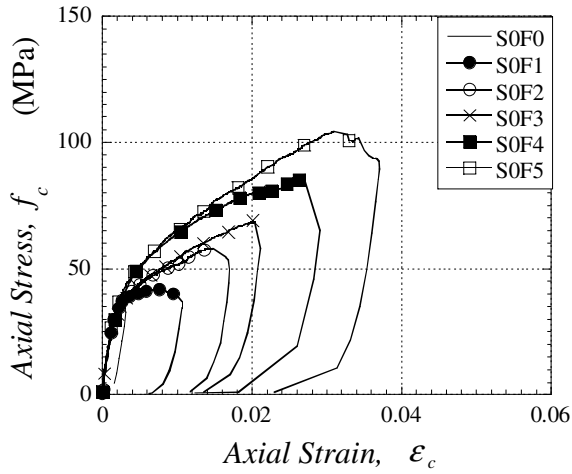


Fig.5 Locations of strain gauges

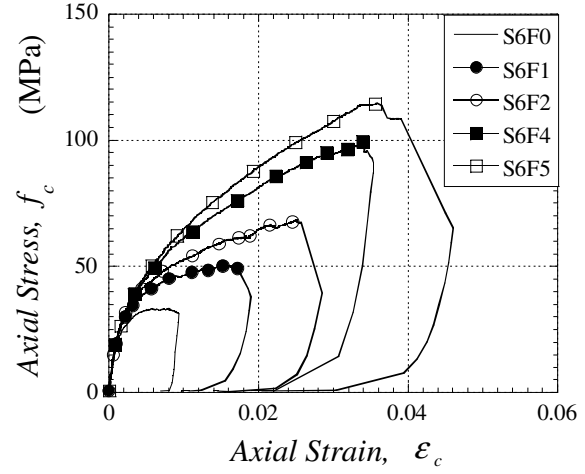
TEST RESULTS

The axial compression stress-strain curves of the 24 RC cylinders are shown in Figs. 6 (a) through (d). The test results of specimen S6F3 are not shown due to errors in the data logger. The figures show that when concrete is still in the elastic stage, the stiffness of unconfined and confined concrete is almost identical. In this stage, the axial compressive strain is still relatively small and in turn the resulting lateral strain is even smaller to engage FRP or steel ties to be effective as confining materials. Once the stress-strain curve of concrete becomes nonlinear, the strength of concrete is found to increase as the amount of FRP wrapping increases and as the pitch of the steel spiral ties decreases.

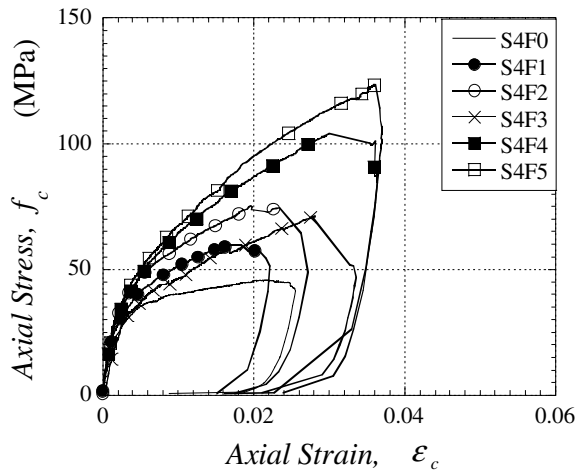
Referring to Fig. 6 (a), the compression strength and the corresponding strain were found to increase as the thickness of the FRP sheets increases. On the other hand, when concrete is confined by both steel spirals and FRP sheets, it was found that the compressive strength and corresponding strain do depend on the thickness of FRP sheets (or number of layers) as well as the volume of spiral ties.



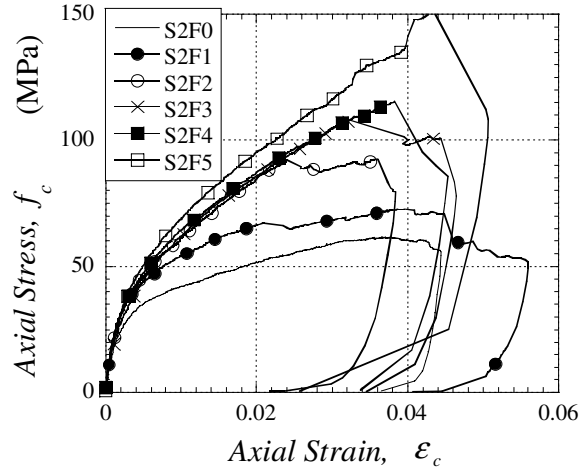
(a) S0 series



(b) S6 series



(c) S4 series



(d) S2 series

Fig. 6 Axial stress-axial strain curves of test concrete cylinders

Table 3 shows the compressive strength and the maximum strain of the test cylinders. While the compressive strength of the confined concrete increases almost proportionally with increasing the lateral confining pressure, the maximum strain does not increase proportionally to f_l , but depends on the ratio of f_{ls} to f_{lf} . The observed increase in axial strain over the unconfined cylinder ranged from 417 to 1292 percent for the CFRP-confined specimens in the S0 series, whereas from 1583 to 1792 percent for the both material-confined specimens in the S2 series. In Table 3, f_{cu} is the compressive strength of specimen, ϵ_{cu} is the maximum axial strain of cylinder corresponding to f_{cu} , ϵ_{co} is the compressive strain of unconfined concrete corresponding to f_c' .

Figure 7 shows the axial stress versus the lateral strain curves of the test cylinders. The figure shows that the lateral strain(ϵ_l) suddenly increases after the axial stress of the cylinder arrives at the compressive strength of unconfined concrete ($f_c'=36.2MPa$). The slope of the curve after $f_c'=36.2MPa$ increases proportionally to the lateral confining pressure. The maximum lateral strains of the cylinders, that have more f_{lf} than f_{ls} , was almost the same as $\epsilon_l \approx 0.011$ regardless of the thickness of CFRP sheets, whereas the maximum lateral strains of the specimens, S6F0, S4F0, S2F0, S2F1, and S2F2, that have more f_{ls} than or similar to f_{lf} , were much greater than 0.011.

Table 3 Compressive strength and maximum strain of the tested concrete cylinders

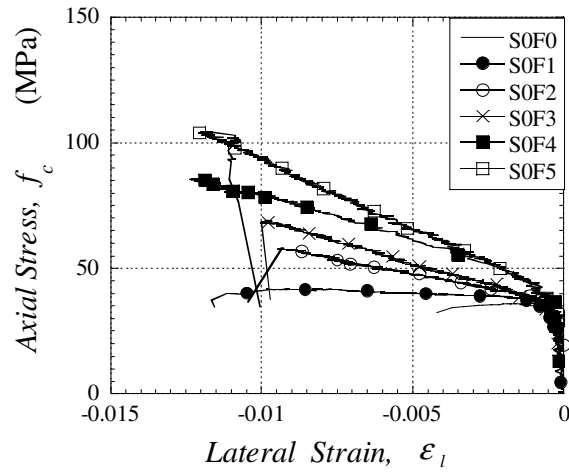
Specimens	f_{cu} (MPa)	ϵ_{cu}	f_{cu} / f_c'	$\epsilon_{cu} / \epsilon_{co}$
S0F0	36.2	0.0024	1.00	1.00
S0F1	41.7	0.010	1.15	4.17
S0F2	57.8	0.015	1.60	6.25
S0F3	69.1	0.020	1.91	8.33
S0F4	85.4	0.027	2.36	11.25
S0F5	104.3	0.031	2.88	12.92
S6F0	33.57	0.008	0.93	3.33
S6F1	50.37	0.017	1.39	7.08
S6F2	68.52	0.025	1.89	10.42
S6F4	99.49	0.034	2.75	14.17
S6F5	114.64	0.036	3.17	15.00
S4F0	45.77	0.022	1.26	9.17
S4F1	60.00	0.019	1.66	7.92
S4F2	74.77	0.023	2.07	9.58
S4F3	73.85	0.029	2.04	12.08
S4F4	104.15	0.030	2.88	12.50
S4F5	123.64	0.036	3.42	15.00
S2F0	61.50	0.038	1.70	15.83
S2F1	72.87	0.039	2.01	16.25
S2F2	92.68	0.036	2.56	15.00
S2F3	108.01	0.039	2.98	16.25
S2F4	115.72	0.038	3.20	15.83
S2F5	150.80	0.043	4.17	17.92

STRESS-STRAIN CURVES OF BOTH MATERIAL-CONFINED CONCRETE

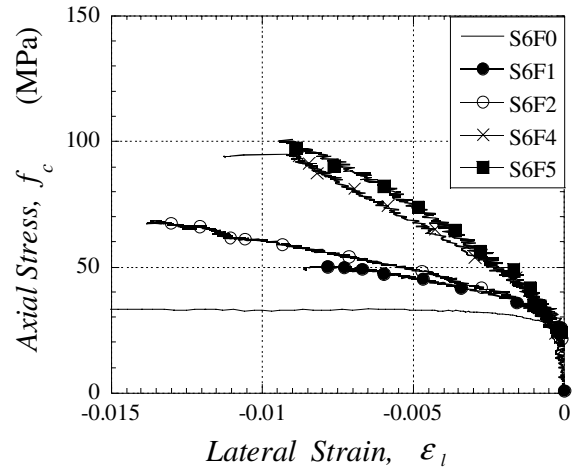
Stress-strain curve of confined concrete

Figs. 8 (a) through (c) should be considered to study the effect of the confinement type (FRP vs. steel spirals) on the compressive axial stress-strain curves of concrete. Fig. 8 (a) shows the compressive stress-strain curves of specimens S0F3 and S2F1. S0F3 is confined only three layers of FRP sheets while S2F1 is confined with both FRP (2 layers) and steel spirals (pitch is 2 cm). The total confining pressure of both considered specimens S0F3 and S2F1 is 21.42 MPa and 19.8 MPa, respectively. This total confining pressure was obtained by simply summing the confining pressure of the FRP composites and the steel spiral ties. Although the total confining pressure was almost the same for considered specimens, Fig. 8 (a) shows that specimen S2F1 exhibited more ductile behavior when compared to specimen S0F3.

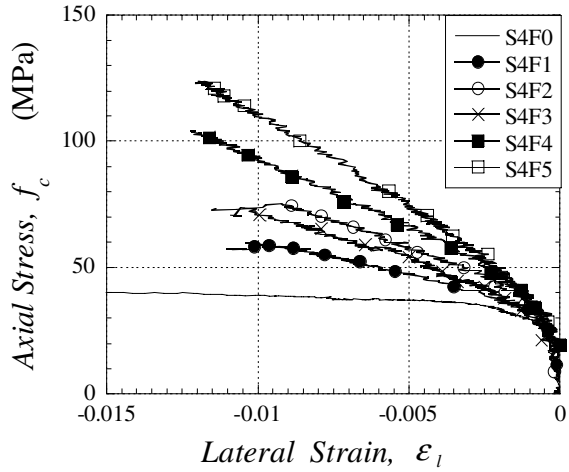
To further study the effect of the confinement type on the compressive stress-strain curve of concrete, Figs. 8



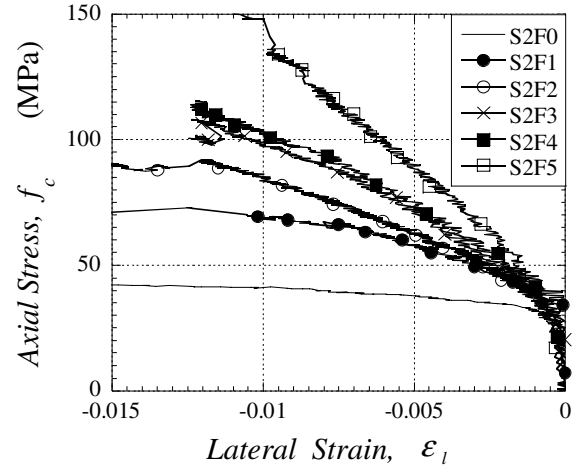
(a) S0 series



(b) S6 series



(c) S4 series

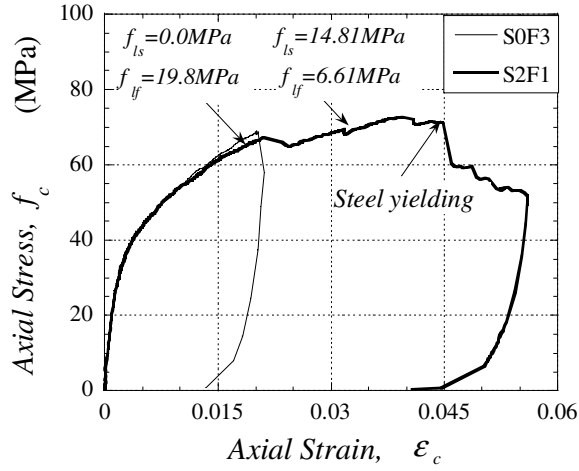


(d) S2 series

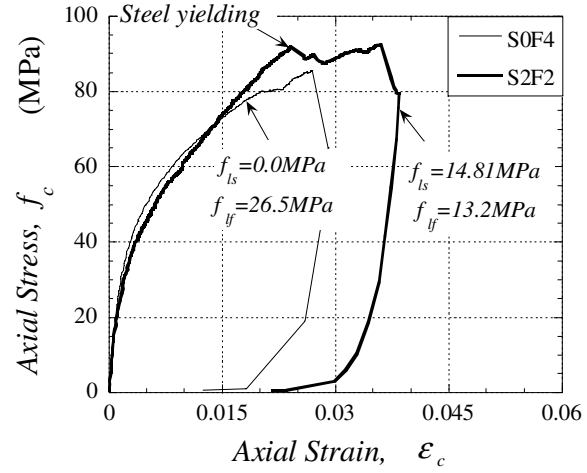
Fig. 7 Axial stress-lateral strain curves of test concrete cylinders

(b) and (c) should be referred to. Here also and similarly to Fig. 8 (a), the specimens considered in Figs. 8 (b) and (c) have almost the same values of total confining pressure. The value of the total confining pressure was almost 26 MPa in Fig. 8 (b) and 33 MPa in Fig. 8 (c). Comparison of Figs. 8 (a) through (c) show that as the value of the total confining pressure increases, the concrete compressive strength increases but the ductility decreases.

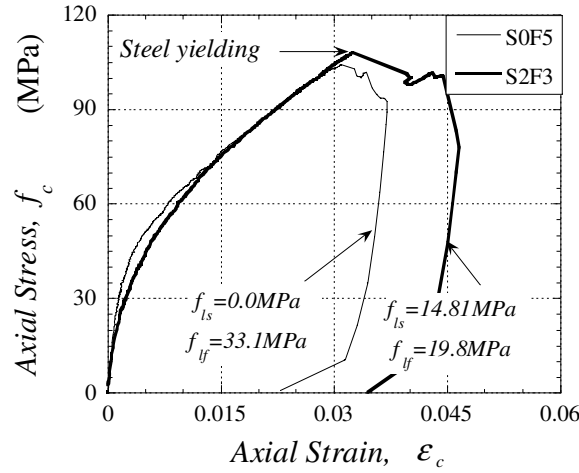
As far as the effect of the type of confining pressure, Figs. 8 (a) through (c) show that higher strength, larger ductility and higher energy dissipation capacity of concrete can be obtained when using both steel spirals and FRP as confining materials.



(a) S0F3 and S2F1



(b) S0F4 and S2F2



(c) S0F5 and S2F3

Fig. 8 Comparison of the axial stress-axial strain curves of cylinders

Compressive strength of confined concrete

Fig. 9 shows the normalized concrete strength of concrete versus the total confining pressure. The normalized strength of concrete was obtained by dividing the concrete strength of each specimen by the concrete strength of specimen S0F0. The figure shows that as the concrete strength increases linearly as the total confining pressure increases.

To further investigate this trend, Fig. 10 shows the compression stress-strain curves of 4 specimens: S0F0, S4F0, S0F4, and S4F4. The strength of specimen S4F0 is larger than S0F0; the difference in strength between these two specimens is denoted by Δf_s in Fig. 10 and represents the increase in strength of specimen S4F0 when compared to S0F0 due to the presence of steel spirals. Similarly, the increase in strength of specimen S0F4 when compared to S0F0 is denoted by Δf_f in Fig. 10, and is due to the presence of 4 layers of FRP material. The figure also shows the increase in strength of specimen S4F4, denoted by $\Delta f_s + \Delta f_f$.

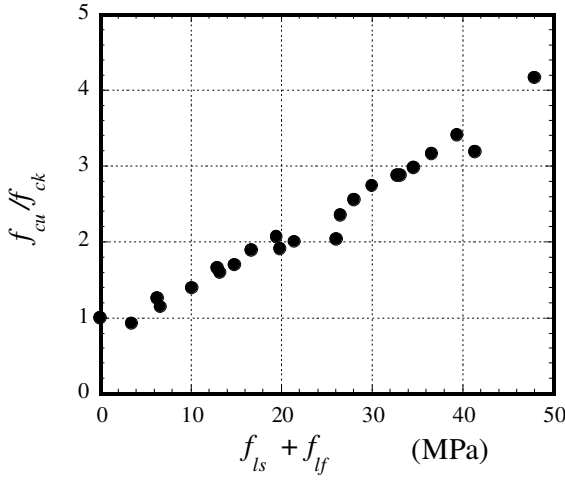


Fig. 9 Compressive strength versus confining pressure of test cylinders curves

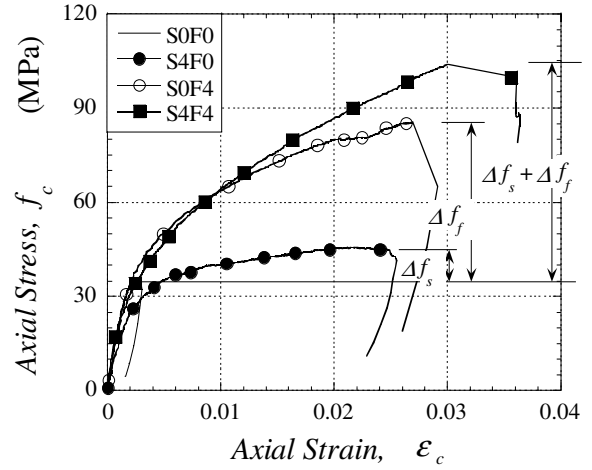


Fig. 10 Comparison of the axial stress-axial strain of cylinders, S0F0, S4F4, S0F4, and S4F4

Maximum compressive strain of confined concrete

Fig. 11 shows the normalized concrete peak cylinder strain versus the total confining pressure. The normalized peak strain of concrete was obtained by dividing the concrete peak strain of each specimen by the concrete peak strain of specimen S0F0. Unlike the linear relationship between the concrete strength and the total confining pressure (refer to Fig. 9), Fig. 11 shows some scatter in the test results.

Thus to study how the confining pressure affect the peak concrete strain, Fig. 12 should be referred to. The figure shows the compressive stress-strain curves of specimens S0F0, S2F0, S0F4, and S2F4. the figures clearly shows that the increase in the peak compressive strain of specimen S2F4 can not be obtained by simply adding the increase in the compressive peak strain of specimen S2F0 to that of S0F4.

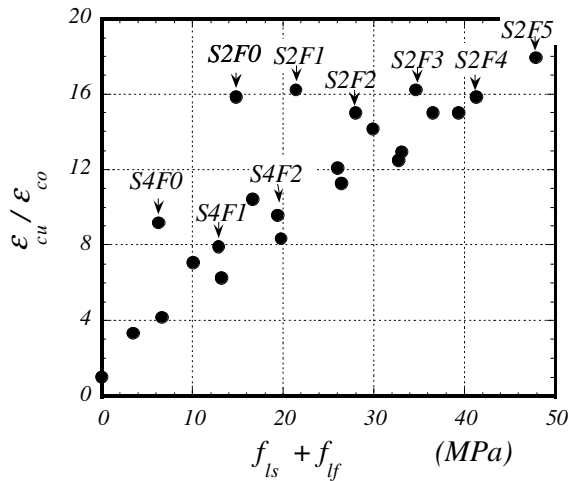


Fig. 11 Maximum strain versus confining pressure strain of test cylinders

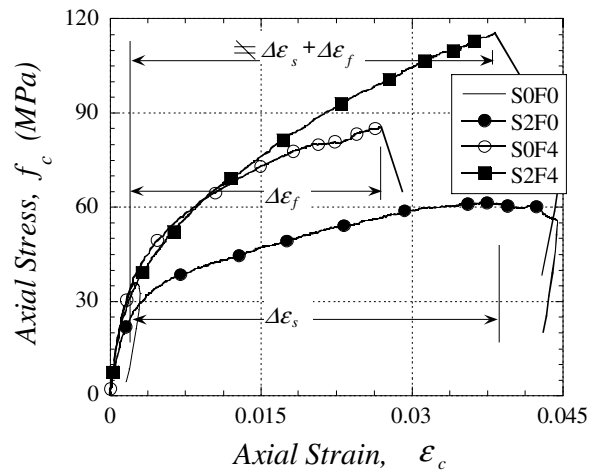


Fig. 12 Comparison of the axial stress-axial curves of cylinders, S0F0, S2F0, S0F4, and S2F4

BEHAVIOR OF CONFINED CONCRETE

Predicting of the stress-strain curve of confined concrete

The behavior of the stress-strain curve of both material-confined concrete is influenced by the ratio of f_{ls} to f_{lf} . The stresses of the cylinders of S0 series and S6 series, that have more f_{lf} than f_{ls} , increase linearly after arriving at the compressive strength of unconfined concrete ($f_c' = 36.2 \text{ MPa}$), and suddenly drops down when CFRP composites rupture. On the other hand, the stresses of the specimens, S4F1, S2F1, S2F2, and S2F3, which have similar amounts of f_{lf} and f_{ls} , increase with little or no increase after the steel spiral yields.

Figure 13 compares the observed stress-strain curve of S2F2, that has $f_{lf} = 14.81 \text{ MPa}$ and $f_{ls} = 13.20 \text{ MPa}$, to the curves calculated by the current models. Mander et al.⁹ proposed Eq.(3) to predict the stress-strain curve of concrete confined with steel spiral.

$$f_c = (f_{cu} \cdot x \cdot r) / (r - 1 + x^r) \quad (3)$$

where $x = \epsilon_c / \epsilon_{cu}$, $r = E_c / (E_c - E_{2m})$, and $E_{2m} = f_{cu} / \epsilon_{cu}$.

The stress-strain curve plotted by Eq.(3) shows that the slope (E_2) of the curve after $f_c' = 36.2 \text{ MPa}$ is almost the same to the second

modulus (E_c) of elasticity of concrete before

$f_c' = 36.2 \text{ MPa}$. However, the E_2 value of CFRP-confined concrete, such as the cylinders of S0 series, is much smaller than the E_c value. Figure 13 shows Eq.(3) based on the test results of steel spiral-confined concrete overestimates the stress of both material-confined concrete after $f_c' = 36.2 \text{ MPa}$. This discrepancy increases as the f_{lf} value increases.

Lam et al.¹² proposed Eq.(4) to calculate the compressive stress-strain curve of FRP-confined concrete.

$$\text{For } \epsilon_t \leq \epsilon_c \leq \epsilon_{cu} \quad f_c = f_{cu} + E_{2l} \cdot \epsilon_c \quad (4)$$

where $\epsilon_t = 2f_{cu} / (E_c - E_{2l})$ and $E_{2l} = 2f_l / \epsilon_{cu}$. To calculate the stress-strain curve of concrete confined with both materials, the sum of f_{lf} and f_{ls} is substituted for f_l . Eq.(4), that was originally proposed to predict the stress-strain curve of FRP-confined concrete, underestimates the stress of both material-confined concrete after arriving at the compressive strength of unconfined concrete, because E_2 of both material-confined concrete, S2F2, is greater than that of FRP-confined concrete. Furthermore, the slope of the curve of S2F2 increases with little or no increases after steel spiral yielded, while the slope of the curve calculated by Eq.(4) increases linearly until CFRP composites rupture as shown in Fig. 13.

Saafi et al.¹¹ predicted the axial stress-axial strain curve of FRP-confined concrete by increasing the lateral strain of concrete (ϵ_l).

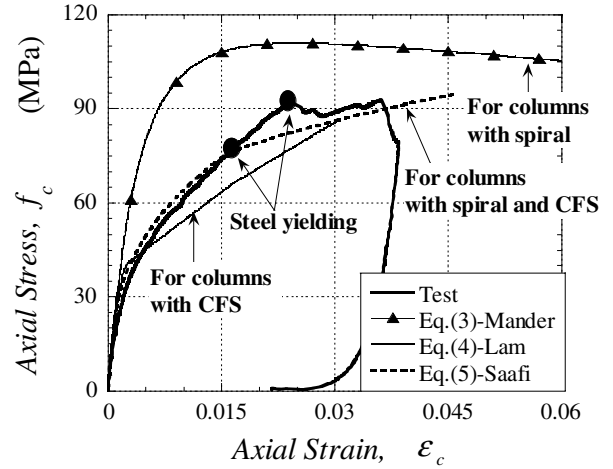


Fig. 13 Comparison between observed and predicted axial stress-axial strain curves

$$f_c = f_c' \left(1 + 2.2 \left(\frac{f_l(\epsilon_l)}{f_c'} \right)^{0.84} \right) \quad (5-1)$$

$$\epsilon_c = \epsilon_{co} \left(1 + (537\epsilon_l + 2.6) \left(\frac{f_c}{f_c'} - 1 \right) \right) \quad (5-2)$$

The first step in the calculation procedures of Eqs.(5-1) and (5-2) involves the selection of the lateral strain of concrete (ϵ_l). The second step involves the calculation of the lateral confining stress (f_l) corresponding to ϵ_l . The stress-strain curves of confining materials, such as steel or FRP composites, obtained from material tests are used to calculate f_l . The third step requires the calculation of ϵ_c and f_c by Eqs.(5-2) and (5-1), respectively. Compared to Eqs.(3) and (4), the calculation procedures of Eqs.(5-1) and (5-2) is more complicate and time consuming. However, because taking into account the characteristics of the stress-strain curves of confining materials, Eq.(5) predicts the stress-strain curve of both material-confined concrete with reasonable agreement as shown in Fig. 13. The slope of the curve calculated by Eq.(5) decreases after steel spiral yields like that of S2F2. Consequently, in order to predict with accuracy the stress-strain curves of both material-confined concrete, there is a need to propose a simple model that includes the characteristics of the stress-strain curves of confining materials.

Compressive strength of confined concrete

The compressive strength of concrete confined with both materials is approximately the same to the sum of the increments of the compressive strength of concrete confined with one material(steel or FRP). Several models were proposed to calculate the compressive strength of confined concrete. Mander et al.⁹ proposed Eq.(6) to predict the compressive strength of spiral-confined concrete.

$$f_{cu} = f_c' \left(-1.254 + 2.254 \sqrt{1 + 7.94 \frac{f_l}{f_c'} - 2 \frac{f_l}{f_c'}} \right) \quad (6)$$

Lam et al.¹² calculated the f_{cu} of FRP-confined concrete using Eq.(7).

$$f_{cu} = f_c' \left(1 + 2 \frac{f_l}{f_c'} \right) \quad (7)$$

Saafi et al.¹¹ proposed Eq.(8) to predict the f_{cu} of FRP-confined concrete.

$$f_{cu} = f_c' \left(1 + 2.2 \left(\frac{f_l}{f_c'} \right)^{0.84} \right) \quad (8)$$

To calculate the f_{cu} of concrete confined with both materials using Eqs.(6) through (8), the sum of f_{lf} and f_{ls} is substituted for f_l in the equations.

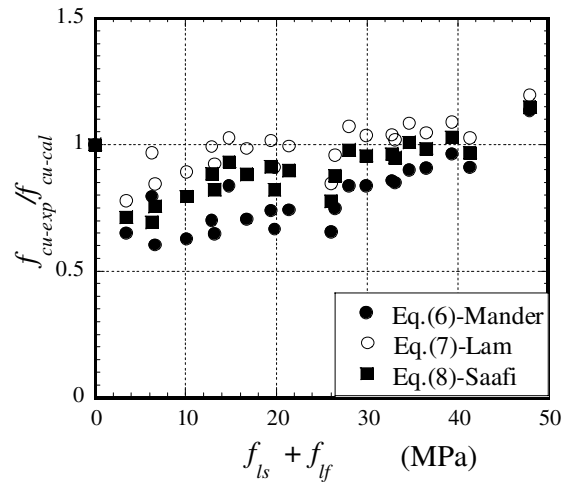


Fig. 14 Comparison between observed and predicted axial strength

Figure 14 show the comparison between the observed shear strength of test cylinders and the calculated

ones by Eqs.(6) through (8). This figure shows the ratio of the experimental compressive strength to predicted compressive strength (f_{cu-exp}/f_{cu-cal}) of the 24 tested cylinders, as a function of the lateral compressive pressure ($f_{ls} + f_{lf}$). The predictions of Eqs.(6) through (8) estimated the observed test results for all values of $f_{ls} + f_{lf}$ with reasonable agreement. The mean values of the compressive strength ratio (f_{cu-exp}/f_{cu-cal}) as given by Eqs.(6) through (8) of the 24 test beams are 0.80, 0.99, and 0.90%, respectively, The variance values of (f_{cu-exp}/f_{cu-cal}) as given by Eqs.(6) through (8) are 17.0%, 9.3% and 12.2%, respectively,

Maximum axial strain of confined concrete

Unlike the prediction of the compressive strength, there is a wide discrepancy between the maximum axial strain(ϵ_{cu}) of both material-confined concrete and the sum of the ϵ_{cu} values of CFRP-confined concrete and spiral-confined concrete as shown in Fig. 11. The ϵ_{cu} value of both material-confined concrete is approximately the same to the larger ϵ_{cu} value between CFRP-confined concrete and spiral-confined concrete.

Mander et al.⁹, Lam et al.¹², and Saafi et al.¹¹ proposed the equations (9), (10), and (11), respectively, to calculate the maximum strain of confined concrete.

$$\epsilon_{cu} = \epsilon_{co} \left(1 + 5 \left(\frac{f_{cu}}{f_c'} - 1 \right) \right) \quad (9)$$

$$\epsilon_{cu} = \epsilon_{co} \left(2 + 15 \left(\frac{f_l}{f_c'} \right) \right) \quad (10)$$

$$\epsilon_{cu} = \epsilon_{co} \left(1 + (537\epsilon_{fo} + 2.6) \left(\frac{f_{cu}}{f_c'} - 1 \right) \right) \quad (11)$$

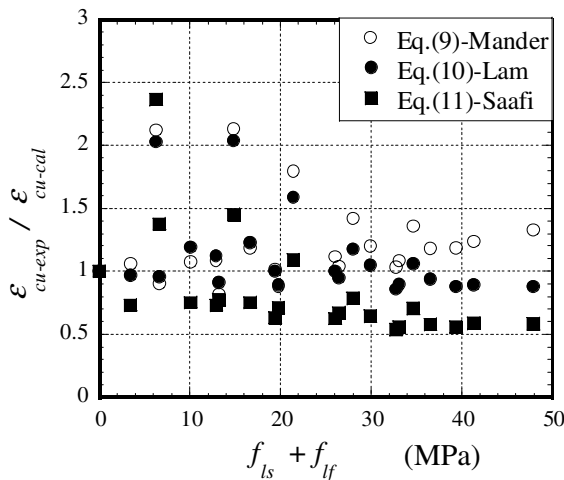


Fig. 15 Comparison between observed and predicted axial strains

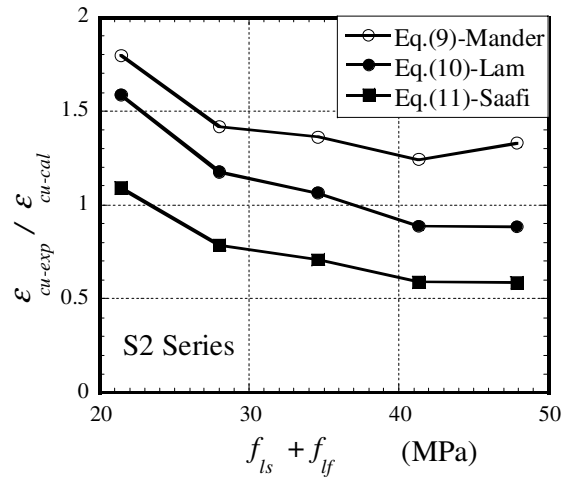


Fig. 16 Comparison between observed and predicted axial strains for S2 series

Figure 15 shows the ratio of the experimental compressive axial strain to predicted compressive axial strain ($\epsilon_{cu-exp} / \epsilon_{cu-cal}$) of the 24 tested cylinders, as a function of the lateral compressive pressure ($f_{ls} + f_{lf}$). The figure shows that the predicted axial strains of Eq.(9) underestimate the observed axial strains for $f_{ls} + f_{lf} \leq 30MPa$. The mean and variance values of the maximum axial strain ratios ($\epsilon_{cu-exp} / \epsilon_{cu-cal}$) of the 24 cylinders as predicted by the Eq.(9) are 1.23 and 28.5%, respectively. On the other hand, the prediction of the maximum axial strain ratio as given by the Eq.(11) not conservative when compared to the results of the Eqs.(9) and (10). The variance values of $\epsilon_{cu-exp} / \epsilon_{cu-cal}$ as given by Eq.(10) and Eq.(11) of the 24 test cylinders are 29.7% and 49.2%, respectively.

This discrepancy between the observed and predicted axial strains is because the ϵ_{cu} value of both material-confined concrete is not the same to the sum of the ϵ_{cu} values of CFRP-confined concrete and spiral-confined concrete, but is influenced by the larger ϵ_{cu} value between CFRP-confined concrete and spiral-confined concrete. Figure 16 shows $\epsilon_{cu-exp} / \epsilon_{cu-cal}$ versus $f_{ls} + f_{lf}$ of the cylinders of S2 series. Even though the $f_{ls} + f_{lf}$ of S2F5 is more than two times that of S2F1, the maximum strains of both cylinders are almost the same. The figure shows that the maximum axial strain ratio ($\epsilon_{cu-exp} / \epsilon_{cu-cal}$) decreases with increasing of $f_{ls} + f_{lf}$.

CONCLUSIONS

In this paper, the behavior of the stress-strain curve of concrete confined with both CFRP and steel spiral was observed by 24 cylinder tests. The observations of the test results led to the following conclusions:

- 1) The maximum axial strain of concrete confined with both CFRP and steel spiral was approximately the same to the larger maximum strains between CFRP-confined concrete and spiral-confined concrete. The current models, that depends on the sum of the lateral confining pressures ($f_{ls} + f_{lf}$), overestimated the maximum strains of the both material-confined concrete when $f_{ls} + f_{lf}$ is high.
- 2) The stress-strain curve of concrete confined with both CFRP and steel spiral was influenced by the ratio of f_{ls} to f_{lf} and the stress-strain curves of lateral confining materials. The slope of the stress-strain curve of both material-confined concrete that had more f_{ls} than f_{lf} decreased after steel spiral had yielded. Thus in order to predict with accuracy the stress-strain curve of both material-confined concrete, it is need to propose a model considering the effects of the ratio f_{ls} to f_{lf} and the stress-strain curves of lateral confining materials.
- 3) The compressive strength of concrete confined with both CFRP and steel spiral was approximately the same to the sum of increments of the compressive strength of CFRP-confined concrete and spiral-confined concrete.

ACKNOWLEDGEMENTS

The writers gratefully acknowledge that this work was supported by Korea Reach Foundation (KRF-2002-003-D00400).

REFERENCES

1. Karabinis AI, and Rousakis TC, "Concrete Confined by FRP Material: a Plasticity Approach," *Engineering Structures* 2002; 24: 923-932.
2. Campione G, and Miraglia N, "Strength and Strain Capacities of Concrete Compression Members Reinforced with FRP," *Cement & Concret Composites* 2003; 25: 31-41.
3. Karbhari VM, and Gao Y, "Composite jacketed concrete under uniaxial compression-verification of simple equations," *Journal of Materials in Civil Engineering*, ASCE, 1997; 9 (4): 185-193.
4. Almad SH, Khaloo AR, and Irshaid A, "Behavior of Concrete Spirally Confined by Fibreglass Filamets," *Magazine of Concrete Research* 1991, 43(156): 143-148.
5. Demers M, and Neale KW, "Confinement of Concrete Columns with Fibre-reinforced Composite Sheets – An Experimental Study," *Canadian Journal of Civil Engineering* 1999; 26: 226-241.
6. Samman M, Mirmiran A, and Shahawy M, "Model of Concrete by Fiber Composites," *Journal of Structural Engineering*, ASCE, 1998; 124(9): 1025-1031.
7. Mirmiran A, and Shahawy M "Behavior of Concrete Columns Confined by Fiber Composites," *Journal of Structural Engineering*, ASCE, 1997; 123(5): 583-590.
8. Richart FE, Brandtzaeg A, and Broun RL, "A Study of the Failure of Concrete Under Combined Compressive Stress," *Univ. of Illinois Engineering Experimental Station, Bulletin No. 185*, 1928.
9. Mander JB, Priestley MJN, and Park R, "Theoretical Stress-Strain Model for Confined Concrete," *Journal of Structural Engineering*, ASCE, 1988; 114(8): 1804-1826.
10. Spoelstra MR, and Monti G, "FRP-Confined Concrete Model," *Journal of Composites for Construction*, ASCE, 1999; 3(3): 143-150.
11. Saafi M, Toutanji HA, and Li Z, "Behavior of Concrete Columns Confined with Fiber Reinforced Polymer Tubes," *ACI Material Journal* 1999; 96(4): 500-509.
12. Teng JG, Chen JF, Smith ST, and Lam L, "FRP-Strengthened RC Structures," *John Wiley & Sons, Ltd*, 2002.